Image fusion between ultrasonography and CT, MRI or PET/CT for image guidance and intervention - a theoretical and clinical study

Caroline Ewertsen

This review has been accepted as a thesis together with four original papers by University of Copenhagen March 6, 2010 and defended on June 18, 2010

Tutors: Michael Bachmann Nielsen and Søren Torp-Pedersen

Official opponents: Andreas Kjær, Anders Magnusson, Steen Karstrup

Correspondence: Department of Radiology, Rigshospitalet, Blegdamsvej 9, 2100 Copenhagen OE

E-mail: caroline.ewertsen@dadlnet.dk

Dan Med Bull 2010;57:(9) B4172

THE FOUR ORIGINAL PAPERS ARE:

1. Ewertsen C, Ellegaard K, Boesen M, Torp-Pedersen S, Nielsen MB. Comparison of two co-registration methods for real-time ultrasonography fused with MRI: A phantom study. Ultraschall Med 2010;31(3):296-301.
2. Ewertsen C, Grossjohann HS, Nielsen KR, Torp-Pedersen S, Nielsen MB. Biopsy guided by real-time sonography fused with MRI: A phantom study. AJR 2008; 190: 1671-1674.
3. Ewertsen C, Henriksen BM, Torp-Pedersen S, Nielsen MB. Image-fusion visualizing liver lesions difficult to see in B-mode. Submitted.
4. Udesen J, Ewertsen C, Gran F, Christensen AF, Kjaer-Kristoffersen F, Engelholm SA, Jensen JA, Nielsen MB. Fusion of 3-D rectal ultrasound with PET-CT. Curr Med Imaging Rev. Accepted for publication 2009.

SUMMARY

The aim of this thesis was to test the clinical application of image fusion involving US.

The first study describes the accuracies of different methods of co-registration in a phantom. The accuracy improved if co-registration was made from points or planes close to the area examined.

The second study describes the accuracy of image-guided intervention on structures invisible to US but visible to CT or MRI. We measured a rate of success of biopsies in a phantom and found a rate of success, similar to that of conventional US-guided biopsy.

In the third study, we found that the number of identifiable lesions by US increased by using the fusion-guided US, and the method was helpful as guidance for contrast-enhanced US (CEUS) as it enabled us to focus on a specific area.

In the fourth study we computed a program to fuse a 3D-US dataset with a PET/CT examination.

We have presented some of the first results on accuracy of real-time image fusion involving US and of the application of the method to patients with liver lesions.

INTRODUCTION

Medical image fusion between different cross-sectional modalities is widely used, mostly where functional images as Positron Emission Tomography (PET) or Single Photon Emission Computed Tomography (SPECT) are fused with the anatomical data of Computed Tomography (CT) or Magnetic Resonance Imaging (MRI). PET/CT has gained widespread use and the two modalities are today incorporated in one system.

The advantages of including ultrasonography (US) in image fusion are the possible higher resolution for high frequency probes, the real-time images and the ease of imaging-guided biopsies or other interventional procedures.

Different mathematical algorithms have been described to include real-time or previously recorded sonograms in image fusion, and different anatomical regions have been studied, e.g., the liver, the prostate and the brain [1-4].

Commercial US systems are now available displaying a previously recorded CT or MRI examination and real-time sonograms simultaneously. The images are shown on split-screen with the possibility of overlaying the images into one single image. The real-time fusion is made possible by means of a magnetic tracking device and specially designed software, which register the scan plane of the US transducer [5,6].

The MRI or CT images are reformatted to fit the live sonograms according to an initial co-registration. Well-defined anatomical planes or points from the images may be used for the co-registration. Few studies have dealt with the accuracy of these commercial systems and their use in humans.

The present PhD-thesis deals with:
The accuracy of different methods of co-registration between US and MRI in a phantom using a prototype US system with incorporated software real-time image fusion.

The rate of success of sonographically guided biopsies of structures invisible to US but visible to CT or MRI in a phantom using a prototype system and a commercially available system for real-time image fusion.

The delineation of liver lesions in patients where malignancy is suspected and the lesions are considered difficult to visualize by US judging from a previously recorded CT or MRI. The delineation by B-mode, fusion-guided US and contrast-enhanced ultrasonography (CEUS) are compared.

The thesis also gives an example of off-line co-registration of static anal endosonograms with PET/CT images.

BACKGROUND

History and physics of Medical Ultrasonography

The interest for the medical use of US developed in the 1950's after US had been used for detection of cracks in metal in aircrafts during World War II [7]. In the 1950's, two-dimensional imaging was possible with static images and in the 1970's real-time scanning and grey-scale display was widely accepted [7]. Since then, the technique has developed into scanners with high frame rates, high spatial resolution and the possibility of using contrast agents.

In physics, the term ultrasound refers to frequencies above human hearing, which means above 20 000 Hertz. However, most commercial medical ultrasound systems work at frequencies between 2-18 MHz. The choice of frequency is a trade-off between spatial resolution and imaging depth: lower frequencies have a higher imaging depth but lower spatial resolution [7,8].

A sound wave is typically produced by means of a piezoelectric crystal, which acts both as a transmitter and a receiver. The crystal is deformed by electrical energy, which generates an electric potential at the desired frequency. This sound wave propagates through the tissues. The tissues absorb a part of the energy, and the rest is partly reflected when there is a change in acoustic impedance of the tissues. Large differences in impedance result in high-amplitude reflections. The reflected echoes are collected by the transducer where the mechanical energy is transformed to electric pulses and a greyscale image is constructed [7-9]. The absorption of energy in the tissues is called attenuation. Attenuation is measured in dB and depends on both the frequency and the distance the sound travels. When creating the images, the ultrasound scanner assumes a constant sound velocity in tissue of 1540 m/s.

US has the advantage of real-time images, lack of radiation and the ability to visualize anatomy in several planes and from different angles.

In order to visualize vascular structures and tissue with different vascularity, contrast enhanced ultrasonography (CEUS) may be used. CEUS is based on microbubbles of a specific gas encapsulated in various types of shells, with diameter sizes between 1 and 7 µm [7,10-12]. In 2009, SonoVue is the most commonly used contrast agent in Europe and European guidelines for the use of it exist [10-15]. Most systems have specific visualization modes for the images of the contrast-enhanced sonograms [7,10-12].

Image fusion involving US

To co-register the images from different imaging modalities, one has to bring the images into spatial alignment, by means of extrinsic or intrinsic markers. Extrinsic markers, known as fiducials in the literature, are placed on the patient to be easily identifiable on the images from all imaging modalities involved. They are easy to use as they are clearly visible, but they have to be placed before the examination and they are often of an invasive character. Non-invasive markers, glued to the skin, are often less accurate [4]. Intrinsic markers are structures (usually anatomical structures) within the patient that can be used as landmarks. The drawback of intrinsic markers is that the landmarks have to be identified by the user, which makes it user dependent.

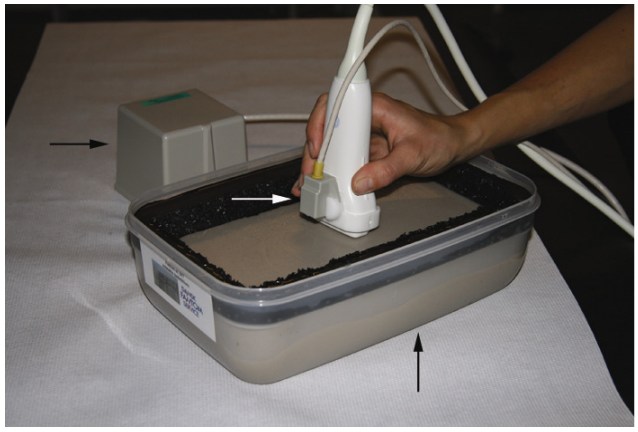

Figure 1
Magnetic tracking system set-up. The magnet (black horizontal arrow) is placed beside the phantom (black vertical arrow). The magnetic sensor (white horizontal arrow) is attached to the transducer.

When identical anatomical structures are marked, a transformation can be performed. Several transformations are available but the most popular in clinical use is based on a rigid-model, assuming that no movements occur within the area of co-registration. It is most commonly used because it is simple and easy to use [4].

Real-time image fusion involving US works by means of a magnetic positioning system, including a magnet placed beside the phantom/patient and a magnetic sensor attached to the transducer and software in the scanner (Fig. 1). This magnetic positioning system enables the system to register the US scan plane and hereby reformat the CT or MRI to that plane. The images are shown on split screen in real-time with the possibility of overlaying the images (Fig. 2). Variable intensity of the images overlaid from two modalities will create a more or less transparent summated fusion image.

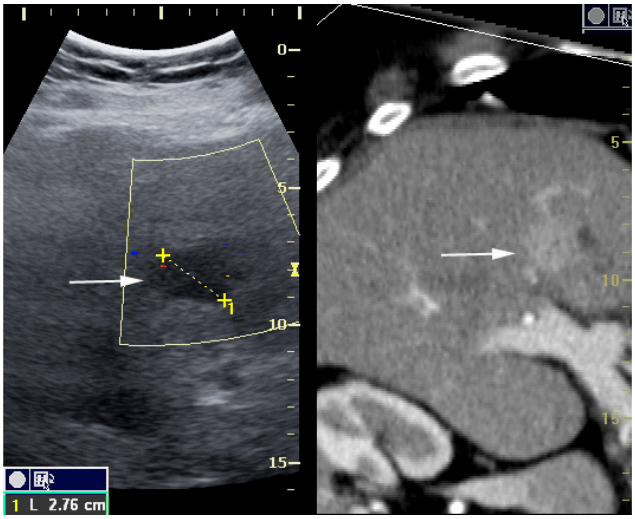

Figure 2
Example of co-registered images. Sonogram to the left – corresponding CT image to the right. White horizontal arrow indicates a liver lesion. Note that the scaling of the images differs.

Off-line fusion refers to previously recorded images from two different data-sets that are co-registered after both data-sets have been obtained, thus not in real-time.

When the studies involved in this thesis were planned in the spring 2006, no papers involving the real-time technique for liver application were available. But image fusion had been used in other anatomical areas as described below.

Endosonography of the prostate and image fusion

Transrectal ultrasonography (TRUS) is used for imaging the prostate gland. In this area, off-line image-fusion between TRUS and CT or MRI has been used for planning of brachytherapy and also for biopsy-guidance, as focal lesions and brachytherapy seeds are better visualized on MRI images. MRI is a more expensive imaging modality and real-time imaging is not widely available [16-19].

Holupka et al. described a real-time ultrasound imaging and targeting system for the treatment of prostate cancer, tested in 13 patients [17]. The patients were scanned with TRUS, then an x-ray was obtained and afterwards a CT-scan with the probe in situ, in order to assess the three-dimensional shape of the prostate. The x-ray image was fused with the TRUS images by using a two-point matching technique and the accuracy of the method was 2 mm.

In a study evaluating prostate seed implants, the CT examination was made with the TRUS transducer in situ in order to co-register the images by means of the transducer. The registration error was less than 1 mm and the co-registered images offered both optimal prostate and seed visibility [19].

Another group tested a system for dynamic dosimetry feedback based on CT-US fusion. They showed a median discrepancy between the images of 0-4 mm and the method improved the position and dose loading of the brachytherapy needles [16].

A TRUS/MRI image fusion was made by Reynier et al. who made the co-registration based on a stepper that gave a constant inter-slice distance of the TRUS images. The volume estimates of the prostate by TRUS compared with MRI showed that TRUS underestimated prostate volume leading to an overestimated brachytherapy dose [18]. Kaplan et al. successfully used real-time fusion for image-guided biopsies in patients with rising prostate specific antigen (PSA). However, the method was only tested in two patients [20].

These promising results from prostate imaging led us to the thought that image fusion between anal endosonograms with the brachytherapy needles in-situ and the CT examination would help in the planning of radiation therapy for anal cancer by making the treatment more precise and focus it on the tumour.

Endosonography of the anorectum

Endosonography of the rectal wall was first described in the 1950's by Wild and Reid [21]. Due to technical limitations, the technique was not introduced into clinical practice for rectal cancer until the 1980's [22]. Usually a high frequency probe of at least 7 MHz, offering sectional views, is used for the examination in order to obtain detailed images of the anal sphincters [23,24].

Anal endosonography is widely used to delineate anal fistulas, visualize deep abscesses and for the preoperative staging of anal or rectal carcinomas [24-27]. Both 2D and 3D endosonography can be used; however, 3D endosonography has been shown to have a significantly better interobserver and intraobserver agreement than 2D endosonography concerning detection of recurrent anal cancer [28].

3D anal endosonography is also used as needle guidance for interstitial brachytherapy seeds, where it optimizes the implant procedure and offers better information for the dose planning [29].

Anal endosonography is used in the primary staging of anal cancer at our institution in combination with digital rectal examination and anoscopy by a surgeon and an oncologist specialized in radiation therapy. It has been shown to improve the diagnostic accuracy and is recommended in the latest guidelines from the National Comprehensive Cancer Network (NCCN) [30]. PET/CT is also used in staging and for the planning of external radiation therapy. All patients initially receive external radiation therapy. Different approaches towards interstitial brachytherapy exist worldwide. At our institution, all patients whose tumour is covering less than half of the circumference are offered interstitial low-dose rate brachytherapy given by a PDR microSelectron (Nucletron)[31]. The size limit is based on the need for preserving the sphincteric functions.

Currently, the radiologist performing the endosonography reports the size of the tumour and the depth of the seeds directly to a physicist, who performs a 3D dose planning based on a CT scan with the applicators in-situ in a BrachyVision (Varian) dose planning system.

Image fusion involving the liver

When we planned our studies, two different commercially systems from Hitachi and Esaote were available. However, none of them were evaluated clinically.

Image fusion involving US used on imaging of the liver was only described in two papers when we planned our studies [32,33]. A method for off-line registration of few US image slices to MRI had been developed, in order to improve the guidance for percutaneous radiofrequency ablation. The method was tested in five volunteers and showed accuracies between 2.3 and 5.5 mm [33].

The other method for image fusion was based on co-registration from vessels in a phantom, and was evaluated in the forearm and in the liver. Co-registration errors depended on the

region studied and in liver ranged between 2-4 mm. This method was also based on off-line registration [32].

Both studies concluded that the fusion of MRI with US was useful for liver biopsy or treatment of liver lesions.

Image fusion involving vessels, heart and lungs

Image fusion has also been applied to other anatomical areas. One of these is as off-line image fusion between x-ray angiography and intravascular US (IVUS), where it has been used to describe plaque morphology in relation to vessel size and curvature in coronary arteries in several studies [34-39]. A system was developed and tested in phantoms, in a porcine model and in humans [36,39]. Plaques seemed to form at the inner vessel walls, where the shear stress is lower. Cothren et al. developed a method for reconstructing normal and diseased coronary arteries from IVUS and bi-plane angiography and successfully tested it both in pigs, and human vessels [34]. They believed the method would be useful in evaluating plaque morphology and assess the impact of pharmacological treatment.

Co-registration of MR angiography with 3D-US of the carotid bifurcation was examined in order to gain better knowledge of this area, because each imaging modality has its limitations regarding plaque morphology [40]. The method was successful with a high accuracy.

To determine the spatial movements of organs by respiration, a system was developed for co-registration of US and CT in order to compensate for these movements in radiation therapy [41]. The system was evaluated in a phantom and had a spatial accuracy of 2 mm, in some cases 1 mm.

It seems cardiovascular and pulmonary studies with image fusion of US are still in their early, less well-validated phase because the studies are small and mainly focused on the technical part of co-registering the images [34-39]. Few studies have dealt with fusion of IVUS and angiography and the clinical indication and the benefit of adding IVUS are not yet established.

Knowledge of the respiratory movements when applying radiation therapy is highly relevant in order to minimize radiation damage. Real-time US saves the patient for the radiation involved in CT [41], thus this area has to be further investigated.

Image fusion in neurosurgery

In neurosurgery, research on fusion of preoperative images with real-time US has been going on for some time. Preoperative CT or MRI images are used for surgical planning and intraoperative US is used for demarcating tumour localization and dissemination. However, the brain shift, which occurs after opening of the dura, makes it difficult to correlate the images.

In order to gain knowledge of the degree of anatomical changes, an image fusion module for CT/MRI and US was developed in image guided neuronavigation [3]. External fiducial markers were placed on the patient's skull before the MRI in order to co-register the images. Several 3D sweeps were performed intraoperatively and the position and orientation of the transducer was tracked by the neuronavigation system. The images were fused postoperatively with a mean registration accuracy of 2.6 mm. Accuracies in the range of 4.1-6.1 mm were believed to represent anatomical shift.

The fusion accuracy of MRI and real-time US has been examined for different distances between probe and object and on different insonating angles in a phantom in order to be able to use the system in neurosurgery [42]. The overall accuracy was 1.08±0.61 mm and the method seemed useful, although interpretation of the images was complicated.

An US device was integrated in a neuronavigation system in order to combine two pieces of hardware in one [43]. Intraoperative US was useful to overcome the inaccuracy caused by brain shift in neurosurgery. The co-registration was made from fiducials placed on the cranial vault. The system could use images of CT fused with MRI, from a planning computer and was tested in 31 patients with intracranial gliomas or vascular pathology. The use of the system led to a better understanding of the anatomical orientation and a better visualization of the brain shift. A comparable system was tested in 23 patients with intracranial tumours with sizes between 1-7 cm [44]. The reported brain shift ranged between 2-25 mm with a mean of 5 mm, depending on the location of the tumours. The conclusion was that control of the tumour resection margin was excellent for metastases, meningeomas and solid gliomas.

In a study on patients with intracranial tumours, intraoperative US fused with preoperative MRI in neurosurgical interventions was compared with US alone [45]. The technique was used in 13 patients and the fused images were judged superior to US alone in all patients examined. Furthermore, it was possible to visualize the brain shift.

Co-registration of US to CT images was also tested in the radiotherapy planning for 3 patients with head and neck tumours and cervical lymph node metastases [46]. The method was regarded as easy with an accuracy of less than 2 mm.

In neurosurgery, promising results for fusing US with CT/MRI were obtained [3,42-46]; however, it is necessary to take the brain shift into account if there is a large mismatch between the co-registered images. By using the method, it is possible to get an idea of the influence from the brain shift and the size of it.

AIMS

Study I concerns the accuracies of different methods of co-registration between US and MRI images in a phantom. Co-registration can be done using either points or planes, which are built-in functions in most commercial systems. The aim of the study was to test the accuracy of point and plane registration in a phantom. Furthermore, to register the time spent on completing a co-registration for two observers, one with prior knowledge to the system.

Study II concerns US-guided biopsies of structures that are only seen on CT or MRI. The aim was to study if biopsy in a phantom using real-time US fused with MRI was possible and to study the rate of success of biopsy on structures invisible on sonograms but visible on MRI.

Study III concerns the application of the real-time method in patients with liver lesions where malignancy is suspected. We investigated if an increasing number of liver lesions became detectable using real-time US fused with CT or MRI compared with B-mode images alone or CEUS.

Study IV concerns the development of a method for off-line image fusion of 3D ultrasound with PET and CT for use in the planning of radiation therapy.

METHODOLOGICAL STUDY, STUDY I: "COMPARISON OF TWO CO-REGISTRATION METHODS FOR REAL-TIME ULTRASONOGRAPHY FUSED WITH MRI: A PHANTOM STUDY"

(Ewertsen C, Ellegaard K, Boesen M, Torp-Pedersen S, Nielsen MB. Comparison of two co-registration methods for real-time ultrasonography fused with MRI: A phantom study. Ultraschall Med 2010;31(3):296-301).
For details please see [47]

Aim

To test the accuracy of point and plane registration in a phantom. Furthermore, to register the time spent on completing a co-registration for two observers, one with prior knowledge to the system.

Materials and Methods

Imaging

We used a prototype LOGIQ US system with a linear probe with a frequency of 12 MHz (GE Healthcare, Chalfont St. Giles, UK) and software for fusion of US with CT or MRI. A tracking system based on a magnetic sensor, attached to the transducer, and a magnet placed beside the phantom, enabled the system to register the spatial orientation of the scanning plane (Fig.1).

MRI of the phantom was performed on an Intera 1.5 Tesla system (Philips Healthcare, Netherlands) with a T1 weighted high-resolution isotropic volume examination (THRIVE). This data set was stored in the standardized DICOM (Digital Imaging and Communications in Medicine) format on a CD and loaded into the US system. Three reference points, A, B, C, were marked on the MRI and also stored in the US system.

Two observers did 30 co-registrations each for each series, adding up to a total of 180 co-registrations. One observer (1) had worked with real-time fusion involving US before, the other (2) had not. Both observers had more than three years' experience with general US.

Image fusion

The phantom (Dansk Fantom Service, Denmark) was designed to give a well-defined number of points and planes. Nine toothpicks were embedded in a box measuring 28.7 x 18.6 x 5.4 cm. The toothpicks had a pick and a string and were placed perpendicularly to each other in the same depth (Fig. 3).

The MRI data set was loaded into the system and displayed as a 3D box beside the live sonogram on screen. Using the trackball, one could rotate or scroll through the entire MRI. Co-registration could be made based on three or more common points (point registration) or by aligning planes (plane registration).

We tested three methods of co-registration: one where the reference points (A,B,C) were used, one where three other points (a,b,c) were used and one where two planes (D,E) were used (Fig. 4). Theoretically, the closer the co-registration points or planes were to the reference points the more accurate the co-registration would appear.

The system was reset after each co-registration to avoid any errors due to accidental movements of magnet or phantom.

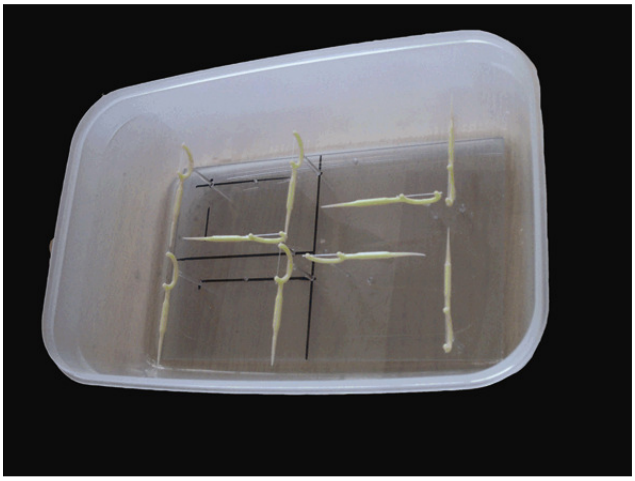

Figure 3
Photograph of the phantom before the phantom substance is added.

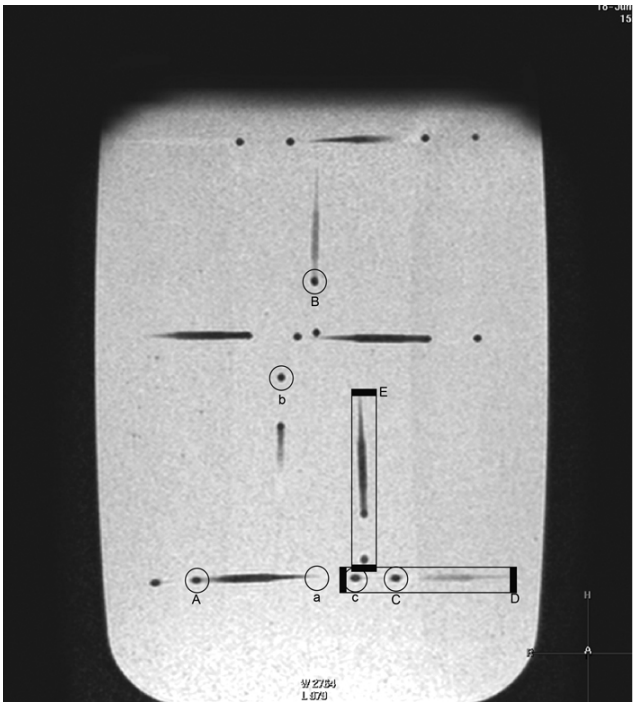

Figure 4
MRI of the phantom, coronal section. Capital letters A,B,C mark the measuring points. In series 1, the points A,B,C were also co-registration points. Letters a,b,c mark the co-registration points in series 2. The boxes D and E mark the co-registration planes in series 3.

Accuracy

Root Means Square Deviation (RMSD) is a well-established method for measuring accuracy of image fusion, as it is the standard deviation of the mean distance between the corresponding registration points on MRI and sonograms.

To allow comparison between series we measured an RMSD ('calculated RMSD') using the points ABC in all cases and thereby also generated a value for the plane registration.

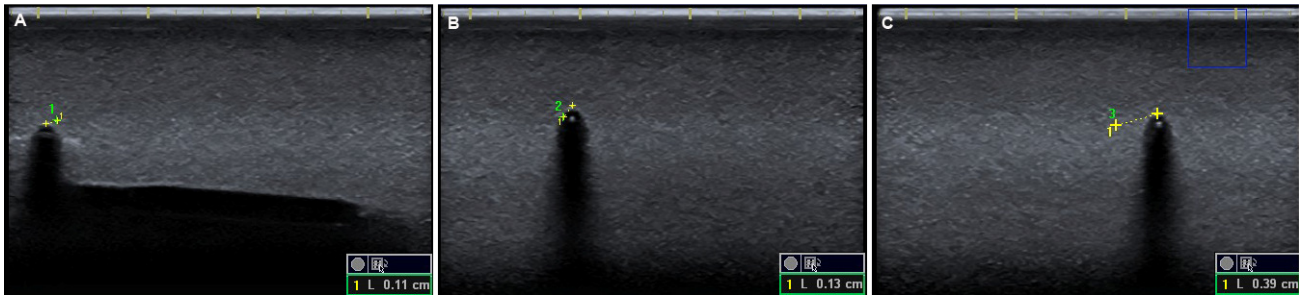

Figure 5
Measuring deviation for RMSD calculation. The measuring points (A,B,C - green) that were stored with the MRI image set were recalled and were displayed as boxes when being outside the image plane, blue box image C (the larger the box the further away the corresponding point was). When the point was in the scanning plane it was displayed as a cursor. The transducer was placed so the cursor and the corresponding point on the sonogram were in the same plane and the image was frozen. The distance was measured from the green MRI-point to the corresponding point on the sonogram.
For the imaged co-registration the average deviation was 0.21 cm and the RMSD-value was 0.25 cm

RMSD in our study is expressed in millimetres (Fig. 5).

Statistics
The statistical software SAS version 9.1, 2002-2003 (SAS Institute), was used for statistical analyses. The significance of the difference between the methods and the observers was calculated using analysis of variance (two-way ANOVA). Data were analyzed using a mixed model without random effects and the 'experience' variable as a fixed effect. RMSD from the equipment was compared with the calculated RMSD using a paired t-test. The significance level was set at 0.05.

Results
In the first series, where co-registration was made at the reference points (A,B,C), the accuracy was significantly higher than when co-registration was done in the other points (a,b,c) or from the planes (D,E) measured by the calculated RMSD ($p<0.0001$). The mean calculated RMSD in the first series was 1.3 mm (95% CI: 1.1-1.5 mm), in the second series 4.0 mm (95% CI: 3.2-4.8 mm), and in the third series 3.8 mm (95% CI: 3.2-4.4 mm) (Fig. 6). Thus, illustrating a deviation between 1.3 – 4.0 mm for the co-registration of corresponding points. The mean reported RMSD from the system was 1.2 mm (95% CI: 1.1-1.3 mm) in the first series, and 0.90 mm (95% CI: 0.8-1.0 mm) in the second series. In the first series, the calculated RMSD did not differ significantly from the reported RMSD ($p=0.22$), but it did in the second series ($p<0.0001$). In the second series the calculated RMSD was higher than the reported. The accuracies (calculated RMSD) of the second and third series were not significantly different from each other ($p=0.12$).

The inexperienced observer (2) had a tendency of improving her accuracy in each series, especially in the second series, where the improvement was significant ($p<0.0001$).

The mean time spent on completing the co-registration was 128 seconds (95% CI: 117-138) for the first series; for the second series 96 seconds (95% CI: 91-101); and for the third series 248 seconds (95% CI: 209-287). There was a decrease in time spent for both observers within each series, especially in the first. There was a trend towards the experienced observer spending less time on the co-registration than the inexperienced observer (data not shown).

Conclusion
Image fusion involving real-time US has a high accuracy and is easy to use in a phantom. Working within the area given by the co-registration points optimizes the accuracy as co-registration from the reference points (A,B,C) was more accurate (RMSD: 1.3 mm (mean)) than co-registration from the other points (a,b,c)(RMSD: 4.0 mm (mean)) or planes (D,E)(RMSD: 3.8 mm (mean)). Accuracy increased and time spent on the co-registration procedure decreased within each series for each observer even though our data could not support a characteristic learning curve.

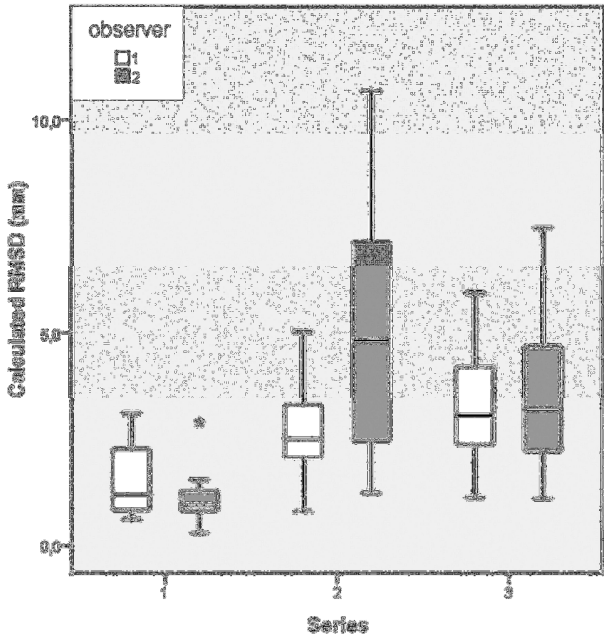

Figure 6
Accuracy (expressed as RMSD) of three different methods of co-registration with 30 observations each series. Boxes show interquartile range with the median marked as a line. Whiskers mark the 2.5 to 97.5 percentiles. Observer 1 has prior knowledge to the system. Observer 2 has not. Outliers are not marked.

METHODOLOGICAL STUDY, STUDY II: "BIOPSY GUIDED BY REAL-TIME SONOGRAPHY FUSED WITH MRI: A PHANTOM STUDY"
(Ewertsen C, Grossjohann HS, Nielsen KR, Torp-Pedersen S, Nielsen MB. Biopsy guided by real-time sonography fused with MRI: A phantom study. AJR 2008; 190: 1671-1674).
For details please see [48]

Aim

To study if biopsy in a phantom using real-time US fused with MRI was possible and to study the rate of success of biopsy on structures invisible on sonograms but visible on MRI**.**

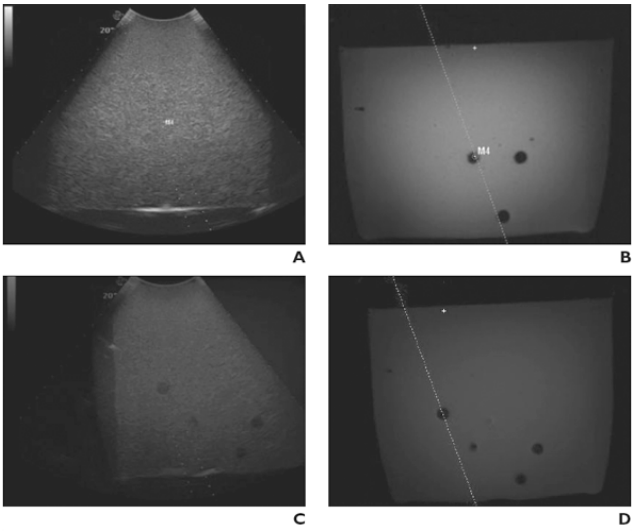

Figure 7
Images of phantom shown on screen. Sonogram (A) and corresponding MRI (B). Target is marked (M4 on B). Overlay on C of MRI (D) and corresponding sonogram. Diagonal line indicates the biopsy guideline.

Materials and Methods

Imaging

We used two different US systems in order to focus on the method rather than on one specific system. One system (system A) was a commercially available system – Mylab70 Xvision (Esaote, Genova, Italy), the other (system B) a prototype LOGIQ system. We used a convex-array probe with a frequency between 2-5 MHz, abdominal preset and needle guidance for both systems.

Three physicians with more than three years' experience with US took 30 biopsies each using system A. Two of these physicians took 20 biopsies each using system B.

MRI was performed on a 3 Tesla Magnetom Trio (Siemens Medical Solutions, Germany). A T1-weighted 3D gradient-echo sequence was performed with a slice thickness of 1 mm. This data set was stored in DICOM format on a CD and loaded into the US system.

Phantom

We used a modified version of model 373 (Dansk Fantom Service, Denmark), as it contained spheres visible or not visible to US (Fig. 7). All spheres were visible on CT and on MRI. The phantom was an 18 x 18 x 15 cm block consisting of a central and a peripheral part. In each corner of the peripheral part of the phantom a sphere visible to US was placed in different depths. Also, to define the central part of the phantom a 1.5 mm copper thread was placed in each corner of the central part. These copper threads and the spheres in the peripheral part were used to co-register the images.

In the central part ten spheres invisible to US were placed in different depths. They contained barium sulphate, which made them visible on CT and ferric oxide, which made them visible on MRI and added red colour to the inside of them. The colour was visible in the biopsy core when the sphere was biopsied correctly (Fig. 8). Leakage was not possible as the colour was not liquid. The diameter of the spheres was 1 cm.

For technical reasons only six of the ten spheres within depths of 10 cm were used as targets. The remaining four were placed too close to the sides of the box to leave room for the needle guidance. In total, 12 spheres were hit successfully 130 times, with a varying number of attempts for each hit.

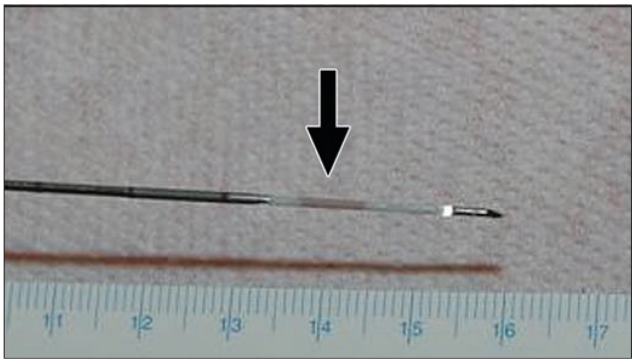

Figure 8
Successful biopsy. Needle has open biopsy chamber containing white biopsy core with central red part (arrow) showing that lesion has been hit. Scale is cm.

Image fusion and biopsy

Identifying a common scanning plane made the initial co-registration. Afterwards the spheres in the peripheral part and the copper threads in the central part were used for the co-registration.

An overlay between the sonogram and the MRI image, which enabled us to see the spheres on the MRI and the needle on the sonogram, was chosen. The systems displayed the percentage of overlay between the images but the scaling differed between the two systems.

We used a semiautomatic biopsy needle 18 gauge x 16 cm (TZ, Gallini Medical Devices). A biopsy was successful if red dye was visible in it. The biopsy procedure on each sphere was continued until the biopsy contained red dye. The number of needle passes and the time spent on the procedure (except from the initial co-registration) were registered. Each sphere was biopsied several times from different angles to avoid air traces from a former biopsy.

Statistics

The statistical software SAS version 9.1.3 2002-2003 (SAS institute) was used for statistical analyses. The median number of attempts and median time spent were calculated. The significance of the variation between the two systems and between the physicians was calculated using a general model based on the Poisson distribution. The significance level was set at 0.05.

Results

It took approximately 10 minutes to load the MRI data set and perform the co-registration. Each sphere was hit several times from different angles to avoid air traces from previous biopsies. 90 targets were hit using system A and 40 targets using system B, making a total of 130 targets.

The median time spent on each biopsy session was 2 minutes (range, 1-15 minutes) after the co-registration. The median number of needle passes on one sphere until at successful biopsy was obtained was one (range, 1-7). Only one biopsy needed 7 attempts, which was due to the needle being caught in previously made needle tracks.

Ninety-four of the 130 biopsies (72.3%) were successful on the first needle pass, 20 of the 130 biopsies (15.4%) were successful on the second needle pass, eight of the 130 biopsies (6.2%) were successful on the third needle pass, and eight of the 130 biopsies (6.2%) were successful after 4-7 needle passes. The distribution of the number of needle passes for the three physicians and the two different systems are shown in Table 1. There was neither a statistically significant difference between the physicians nor between the systems (range of p values, 0.43-0.81).

Table 1
The distribution of the number of needle passes for the three physicians and the two different systems.

System	No. of successful biopsies	No. of needle-passes to obtain sucessful biopsy Median (range)	Time spent per biopsy target (min) Median (range)
A Physician 1	**30**	**1 (1-3)**	**2 (1-5)**
Physician 2	**30**	**1 (1-5)**	**2 (1-7)**
Physician 3	**30**	**1 (1-7)**	**2 (2-15)**
B Physician 2	**20**	**1 (1-4)**	**1 (1-6)**
Physician 3	**20**	**2 (1-5)**	**2 (1-11)**

Conclusion

Image fusion between real-time US and MRI was successful in obtaining an adequate sample of lesions not visible to US but visible to MRI in a phantom. The rate of success was in accordance with conventional US-guided biopsies. In our department two needle passes are usually spent in the clinical routine.

The method was safe to continue with patient studies.

CLINICAL STUDY, STUDY III: "IMAGE FUSION VISUALIZING LIVER LESIONS DIFFICULT TO SEE WTIH B-MODE ULTRASONOGRAPHY"

(Ewertsen C, Henriksen BM, Torp-Pedersen S, Nielsen MB. Image-fusion visualizing liver lesions difficult to see in B-mode ultrasound. Submitted).

Aim

To investigate if an increasing number of liver lesions became detectable using real-time US fused with CT or MRI and CEUS compared with B-mode images alone.

Materials and Methods

Patients

Forty patients referred to diagnostic US evaluation or US-guided biopsy of liver lesions seen on CT (N=35), MRI (N=2) or PET/CT (N=3) and where malignancy was suspected were prospectively included in the study. Focus was on patients where the lesion could be difficult to see by US judging from the CT, MRI or PET/CT. This could be due to poor delineation or to location near the diaphragm. If a patient had several lesions only one lesion was included in the study.

Twenty-eight males and 12 females with a median age of 64 years (interquartile range: 54-69) were included.

Final diagnoses of the patients, where the pathology description was inconclusive or where the lesion remained invisible with fusion-guided US and CEUS, were found in their medical records after 10-275 days.

Imaging

We used at LOGIQ US prototype system with incorporated software for fusion imaging, US and MRI or CT (GE Healthcare, Chalfont St. Giles, UK). We used a convex-array 4 MHz transducer with abdominal setting (GE Healthcare, Chalfont St. Giles, UK). Needle guidance was attached to the system when a biopsy was needed. The images were shown on split screen with the possibility of overlaying the images (Fig. 9).

A CT or MRI had been recorded previously for all patients. For some patients contrast-enhanced ultrasonography (CEUS) was used. The contrast agent was Sonovue (Bracco, Italy) in a dose of 2.4 ml, which could be repeated. The contrast-enhanced sonogram (sonogram in contrast mode) was shown on split screen with either the B-mode sonogram or the reformatted CT image.

One consultant in radiology specialized in US and one physician with more than three years' experience with US did the examinations.

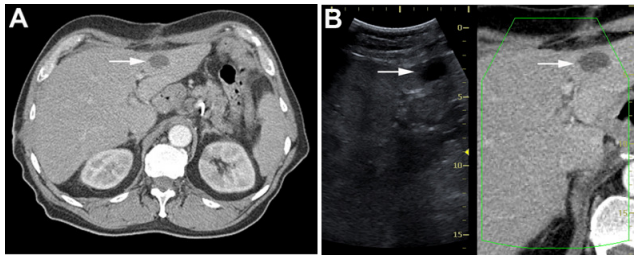

Figure 9
CT and fusion-guided US images in a patient with suspected metastases from cardia cancer and a cyst in the left lobe of the liver. A. CT image, transverse section through the liver. White horizontal arrow indicates the cyst in A and B. B. Co-registered images from fusion-guided US in transverse section. Sonogram to the left and reformatted CT image to the right. The green box indicates the area of the sonogram.

Image fusion

All patients were examined in the supine position with their right arm resting over their head or on the chest to mimic the situation in the CT-/MRI- setting. The magnet from the magnetic tracking system was placed on the patient's left side close to the hipbone pointing towards right shoulder.

A transverse plane including the upper mesenteric artery, the aortic bifurcation or the umbilicus was used for the initial co-registration depending on the overview.

Afterwards confluences of hepatic veins or bifurcations of portal veins in the area of interest were used to co-register the images. A minimum of three common points was selected.

For biopsies, either fine needle aspiration (FNA) 0.7 mm or core biopsies (CB) 1.2 mm were obtained preceded by subcutaneous analgesic by lidocaine.

Statistics
The difference in tumour size between visible and invisible tumours was analyzed using non-parametric statistics due to lack of Normal distribution. Sensitivity, specificity, positive predictive value and negative predictive value were calculated. All statistical analyses including descriptive statistics were done using the statistical software package SPSS 16.0 (SPSS Inc.).

Results
Twenty-six lesions were initially invisible with US. Of the 26 lesions, which were invisible in B-mode, 9 became visible with fusion-guided US (35%) and another 4 (15%) became visible with CEUS in combination with fusion-guidance (Table 2).

Table 2
Distribution of visibility with either modality for the patients included in the study.

- 40 lesions
  - 14 visible in B-mode
  - 26 invisible in B-mode
    - 9 visible with fusion-guided US
      - 4 visible with CEUS
      - 2 invisible with CEUS
      - 3 did not receive CEUS
    - 17 invisible with fusion-guided US
      - 4 visible with CEUS
      - 10 invisible with CEUS
      - 3 did not receive CEUS

Tumour size did neither predict the US visibility of lesions in B-mode nor the visibility with guidance from CT/MRI for these tumours.

The median tumour size for all lesions included in the study was 1.5 cm (interquartile range: 1.0-2.4; N=40). There was no statistically significant difference in size for the B-mode and CT/MRI guided invisible lesions.

In 21 patients a biopsy was taken, 17 CBs and 4 FNAs.

Because all patients included in the study had a history of suspected or confirmed malignancy, the interpretation of the US was less likely to exclude malignancy.

Conclusion
We have successfully demonstrated an increase in the delineation of liver lesions by using fusion-guided US compared with conventional B-mode US.

Thirty-five percent of B-mode invisible lesions became identifiable by using the method and another 15% became visible by adding CEUS.

Fusion-guided US improved the CEUS in 21 cases regardless of whether the lesion was visible or not. It enabled us to focus on the area with the suspect lesion, because the reformatted CT or MRI image was shown beside the sonogram in contrast mode. Hereby we could focus on that area, knowing that the lesion should be in the scanning plane. Because fusion-guided US is more time consuming than an ordinary US examination, the method should be reserved for patients with difficult lesions.

CLINICAL STUDY, STUDY IV: "FUSION OF 3-D RECTAL ULTRASOUND WITH PET-CT"
(Udesen J, Ewertsen C, Gran F, Christensen AF, Kjaer-Kristoffersen F, Engelholm SA, Jensen JA, Nielsen MB. Fusion of 3-D rectal ultrasound with PET-CT. Curr Med Imaging Rev. Accepted for publication 2009).

Aim
To develop a method for off-line image fusion of 3D ultrasound with PET and CT for use in the planning of radiation therapy.

Introduction
As a model we used 3D anal endosonograms in patients with anal carcinoma. When we planned the study the external radiation therapy was planned from a CT scan in combination with a description of the 3D anal endosonograms. On the CT scan, the tumour would be unclearly demarcated due to the low contrast resolution in this area [49,50]. We believed that importing the initial 3D anal endosonogram into the dose-planning program would help the planning of the external radiation therapy. Shortly after we initiated the study, PET/CT replaced CT for the planning of external radiation therapy. Then we decided to import the 3D anal endosonograms with the brachytherapy needles in-situ, into the dose-planning program, in order to make the radiation therapy more precise.

When we planned the study no DICOM standard for 3D anal endosongraphy existed and no commercial software for involving US in image fusion was available. In the DICOM format information is grouped in data sets so the patient ID, type of scan, image dimensions etc. are contained within the image file. In order to import the 3D images we had to split the 3D block of images into separate files and add a DICOM header by means of a Matlab (MathWorks, Massachusetts) code. Hereby we could import all the images from the 3D US block to the dose-planning program. Afterwards the Matlab program, described below, for fusion of US with CT and PET was coded.

Materials and Methods
A semi-automatic algorithm was implemented in an in-house Matlab program (MathWorks, Massachusetts). A manual co-registration was made based on the identification of a perspex rod, placed endorectally during the PET/CT examination, the rectal endoprobe and two points chosen by the physician.

The three fused imaging modalities US, PET and CT were shown in three orthogonal slices. Opacity, colour map, slice location and viewpoint could be changed dynamically to choose the optimal set-up (Fig. 10).

The method was tested using a B-K Medical US system 2102 (B-K Medical, Herlev, Denmark) with built-in 3-D mode, and a 10 MHz rotating endoprobe.

PET-CT was performed on a Siemens Biograph 16 scanner (Siemens, Erlangen, Germany). The patient had a perspex rod with the same physical dimensions as the US transducer inserted into the anal canal during the PET-CT examination. The images obtained from a 65-year-old man with anal cancer were used to test the method.

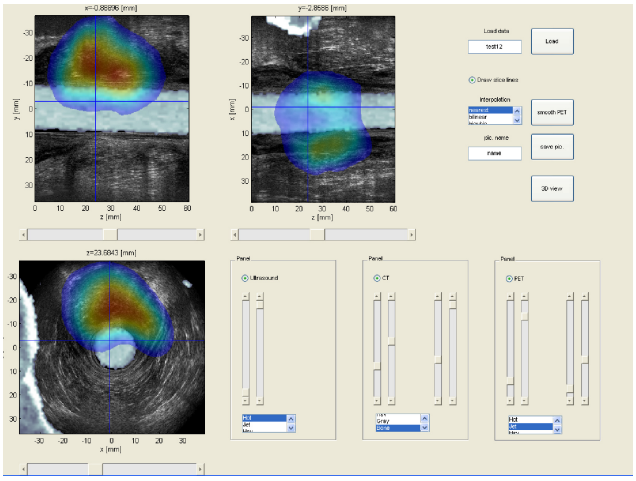

Figure 10
The three orthogonal planes shown on screen in the off-line in-house program, where opacity can be adjusted.

Results

The algorithm resulted in a successful transformation of the PET/CT images to the US images. An example where the perspex rod is transformed precisely from the CT image to the US image. The corresponding PET image is shown with a blue-yellow-red colour-map.

Different visualization approaches can be implemented to present the fused 3-D PET-CT-US images (Fig. 11).

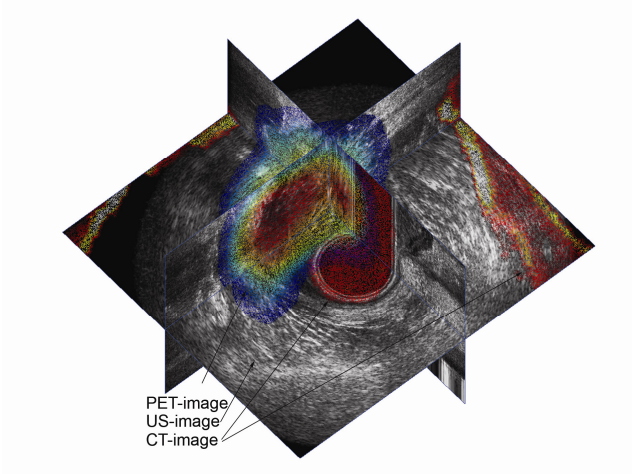

Figure 11
One way of displaying successful image-fusion of US, CT and PET.

Conclusion

Off-line fusion of three imaging modalities by means of a semi-automatic algorithm was possible with the in-house program. As mentioned in the introduction and in the discussion, PET/CT replaced US for the planning of the external radiation therapy and for the interstitial brachytherapy the original tumour volume had to be irradiated. Therefore the program was never tested clinically.

DISCUSSION

New achievements

We have measured the accuracy of point and plane co-registration in image-fusion involving real-time US. We found an accuracy of 1.3 mm in an optimal setting for this method: a stationary phantom with several well-defined points and planes. Thus, real-time fusion involving US appears equally accurate to static fusion systems. We found that co-registering close to the points of interest improves the accuracy, and in our setting that was in the points used for measuring the accuracy.

We successfully showed that biopsy of lesions invisible to US but visible on MRI and CT was possible in a phantom with a rate of success comparable to conventional US-guided biopsy.

We also demonstrated an increase in the identification of liver lesions by using fusion-guided US compared with conventional B-mode US. Of the 26 lesions, which were invisible in B-mode, 9 became visible with fusion-guided US (35%) and another 4 (15%) became visible with CEUS.

We also succeeded in making off-line fusion of 3D anal endosonograms with PET/CT and successfully imported a 3D block of anal endosonograms into a commercial dose-planning program (Eclipse). However, due to current guidelines this method was never clinically tested.

Accuracy of co-registration

The accuracy refers to the “true” error occurring at a specific image location and can occur at many levels phantom, pre-clinical and clinical [4].

When planning our studies, we decided to measure accuracy as Root Mean Square Deviation, RMSD, a well-established method for measuring accuracy of a co-registration between different imaging modalities [2,33,46,51,52]. The calculation of RMSD is made from the formula:

$$\text{RMSD}=\sqrt{\frac{\sum_{i=1}^{n}(x_{1,i}-x_{2,i})^2}{n}}$$

Where n : number of point pairs, $x_{1,i}-x_{2,i}$: the distance between the corresponding point from two different data sets, when they are superimposed.

Mathematically, the RMSD value of point distances in the matching algorithm is the result of a minimization process. If at least 3 point-pairs are set, the coordinate system of the volume dataset is translated and rotated in space in such a way that the sum of the squared distances of the point pairs is a minimum [53].

Our system reported an RMSD measured in cm after the co-registration had been made from points. In all our studies, we have observed that even though the system reported a low RMSD the fused images could deviate in several planes when focusing on a specific area of interest. In our phantom study (study I), we noticed the difference between the calculated RMSD and the RMSD reported by the system, which was due to the minimization process. The deviation would enlarge when moving away from the co-registration points. In the patient study we did not have an exact measure of the phenomenon, but it occurred in varying degree from patient to patient depending on how close to the area of interest the co-registration could be made.

Accuracy in comparison with reference modalities

The most common use of image fusion is probably between anatomical images as CT and functional images from PET or SPECT, which are widely available and today are incorporated in PET/CT or SPECT/CT systems. Also very recently PET/MRI has been introduced [54-56]. Lavely et al. tested the accuracy of PET and CT co-registration in a phantom and patient images [57]. They concluded that the registration accuracy decreased as distance from the initial registration points increased. We observed the same in our phantom study (study I) where the accuracy decreased from 1.3 mm (1.1-1.5 mm) to 4.0 mm (3.2-4.8 mm) as the distance between the co-registration points and the measuring points increased. Lavely et al. had overall accuracies of < 2mm in the phantom and < 4mm in the patient images.

Förster et al. compared the accuracy using both internal and external markers for the co-registration of abdominal SPET/CT images [53]. They found that external markers were easier and faster to use than internal markers, and that the mean deviation between corresponding points was smaller for external markers (4.17±0.61 mm) compared with internal markers (6.47±1.37 mm).

From these studies it seems that the accuracies from our phantom study (study I) are comparable to accuracies measured for PET/CT or SPECT/CT, where the images are obtained in sequence with the patient remaining on the examination bed.

We have only used internal markers for our co-registrations for several reasons. One was due to logistics. Most of our patients had their CT done for diagnostics or for follow-up of neoplastic disease. Therefore it was unknown when the CT or MRI was recorded whether there would be a new lesion or not, making markers unnecessary in a several patients. There was also a time span until the US examination was carried out, making external markers unreliable, as one could not be sure that they would remain in the right place. As we did not know which patients would need the US examination, it would be impossible for the patients to keep external markers attached to their skin between the CT and the US examination. Furthermore, several anatomical landmarks were available in the liver for the co-registration.

We did not measure accuracies in our patient study (study III), but we noticed that the co-registration was improved if the corresponding points for the co-registration were marked in the same respiratory phase - in our case deep inspiration, as the CT images were acquired in this respiratory phase. Several groups describe problems from the movement of organs caused by respiration [53,58,59]. Goerres et al. showed differences of up to 8 cm in the top of the diaphragm when CT was acquired in maximal inspiration for co-registration of thoracic organs in an integrated PET/CT system [59]. We noticed that the parallel shift occurred in several planes and also implied rotational shifts for the liver, especially the most cranial parts. We did not experience such phenomenon in the phantom studies and hence ascribe this solely to the effect of the respiratory movement.

Our results from the first phantom study (study I) showed accuracies comparable to those measured in PET/CT. This led us to our second phantom study about biopsy (study II) where we obtained high rates of success. From these results we found it safe to continue with the patient study (study III).

Conclusion and comparison with recently published studies

After we initiated our studies, image fusion between real-time US and CT or MRI has been reported by several groups [2,51,60-65]. Two different commercial systems (Hitachi and Esaote) and some experimental systems have been used. Most have dealt with invisible lesions on US either as phantom/ ex-vivo studies in animals [60,65] or patient studies [2,51,61-64]. Hepatocellular carcinomas (HCCs), which can be difficult to delineate on US, were studied in three Japanese papers with varying set-ups [61-63]. The same group produced two of these [62,63] and used a commercial system from Hitachi (Hitachi, Tokyo, Japan) for radiofrequency ablation (RFA) of HCC poorly demarcated on CT.

Outcome was measured as the number of attempts to achieve complete tumour necrosis by US-guided RFA. All studies concluded that the method was efficient but an exact measure of the accuracy was not given.

RFA of "invisible lesions" made by injected lead pellets in bovine livers, was studied by Crocetti et al. [60]. A commercial system from Esaote (Esaote, Genova, Italy) was used. The authors reported a high accuracy, with a mean CT-US registration error of about 3.0 mm in this ideal setting without patient or respiratory movements.

Bovine livers were also used in another study, where real-time fusion of images from ultrasound and a gamma probe were used to localize artificial liver metastases intraoperatively [65]. The "artificial liver metastases" contained Tc-99m and F-18 in order to detect them by a gamma probe and by PET. The authors found a lower rate of false positives by using the technique, but the accuracy was not determined.

In human studies [2,51,64], a new algorithm with an average registration error of 8.1 mm throughout the liver, was recently described by Wein et al. [51,64]. The system worked, as the commercial systems, by means of a magnetic tracking device and was tested in 25 patients with indeterminate lesions in liver and kidney. Krucker et al evaluated an electromagnetic tracking system for interventional procedures guided by CT-US image fusion on 20 patients with abdominal pathology. External markers, fiducials, were used for the co-registration procedure, and the overall accuracy was 5.8 mm +/- 2,6 mm [2].

Image fusion between US and CT or MRI for liver imaging has been applied successfully both off-line and in real-time. Generally, adding multiple imaging modalities improves the diagnostic accuracy also for image-guided interventions. Each anatomical area has its own advantages and drawbacks.

Overall, all studies involving liver or phantoms mimicking liver showed high accuracies and promising results for including US in the image fusion. In liver imaging, several landmarks are available for the co-registration of the images, which could possibly make the co-registration procedure more accurate.

These results correspond well with our results, where we have been able to accurately perform biopsy on structures only visible on CT or MRI in a phantom (study II). We were among the first publishing results about this application. In our patient study (study III), several anatomical landmarks were available for the co-registration procedure, and the image fusion increased the number of lesions, which could be delineated by US.

Reference modalities

Image-guided percutaneous biopsy is a safe, well-established, and widely used procedure [66]. In Europe US-guided biopsies are widely used and in Denmark we have a long tradition for US-guided interventions. Several US-guided interventions were first described in Denmark, among these are: US-guided liver biopsy [67], US-guided kidney biopsy [68], US-guided drainage of a kidney abscess [69], US-guided nephrostomy [70], US-guided celiac axis block [71],US-guided drainage of breast abscesses [72], US-guided transrectal biopsy of recurrent rectal carcinoma [73], US-

guided transrectal and transvaginal catheter placement [74]. US-guidance has had a huge impact on patient management, as it is less traumatic and complications are rare [75,76]. In our department the frequency of US-guidance compared with CT fluoroscopy-guidance is estimated to approximately 20:1, and much higher if only abdominal interventions are considered. In our department CT fluoroscopy-guidance is mainly used for lung or skeletal lesions, where US-guidance is impossible.

Alternatives to US-guided biopsies are CT- or CT fluoroscopy-guided interventions and MRI-guided biopsies. In the United States, CT- or CT fluoroscopy-guided interventions are more widely used than in Europe, probably due to tradition and the shorter learning curve reported [66,77]. CT- and CT fluoroscopy-guided interventions have the advantages of high spatial and contrast resolution and accurate needle tip localization. The methods can be used for biopsy guidance for lesions anywhere in the body [66]. CT fluoroscopy is useful in liver lesions that show transient enhancement with contrast agent or are located close to the diaphragm [78]. In a study by Schweiger et al., sensitivity was 94% and specificity was 92% of CT-guided core needle biopsy in oncology patients [78]. The disadvantage of CT- or CT fluoroscopy-guided interventions is mainly the high radiation exposure also to the operator, thus the method should be reserved for more complicated cases [79].

MRI has the advantage of high-contrast resolution, the ability to visualize vessels without the need for a contrast agent and the lack of ionizing radiation [66,80]. In studies from Stattaus J et al. [81] and Kariniemi et al. [82], high sensitivity and specificity are reported for MRI-guided biopsy in the abdomen and liver both in high and low field scanners. The drawbacks of the method are the long examination time and the need for special biopsy needles, made from a non-magnetic material, which is generally softer than ordinary biopsy needles. This may cause deviation of the needle especially in cirrhotic livers or in deeply lying lesions, in which cases the patient has to be moved in and out of the magnet bore in order to use a stainless steel stylet resulting in an increased examination time [80-82]. Generally, the examination time is longer than CT- or US-guided interventions, and the use of MRI-guidance is recommended only in selected cases, i.e., where US- or CT-guided interventions have been impossible [80-83]. In our department MRI-guided biopsies are only performed in selected cases for breast tumour diagnostics.

US-guided biopsies have many advantages: the real-time imaging, shorter procedure time, portability, lack of ionizing radiation and decreased cost [66,77,84]. US-guided biopsy is first choice in many departments and our results confirm that with the guidance from image fusion, tumour delineation and hereby biopsy will be possible in more cases. Hereby patient and operator will save time. For the cases where the lesion remains invisible by US, CT- or CT fluoroscopy-guided and MRI-guided biopsies should be used.

Patient population in study III

We chose a selected patient group due to several reasons. The most important reason being that US-invisible liver lesions are rare. In this respect we were helped by our hospital's status as a tertiary reference centre with highly specialized departments. In most patients in our hospital, neoplastic disease was present or suspected and there were a high number of these patients in the hospital. Secondly, real-time image fusion was more time-consuming than an ordinary US due to the co-registration procedure and therefore we reserved the method for patients who had lesions that could be difficult to visualize judging from the CT or MRI.

We experienced that an accurate co-registration was more difficult to obtain in obese patients, as we had to apply more pressure to the transducer in order to obtain good images. Hereby the subcutaneous fat and also the organs were displaced in comparison with the previously recorded CT- or MRI-images. For the CEUS examinations, the distance from the skin to the lesion was too long to visualize the microbubbles properly, which explains why one lesion in the patient study (study III) was visible with fusion-guidance and not with contrast-agent. This corresponds well to the current European guidelines for the use of CEUS [13] where it is mentioned that if "the baseline US is suboptimal the CEUS may be disappointing".

The method is highly dependent on patient cooperation for the co-registration procedure. Because some structures are only visible in a certain phase of the respiration and because the respiratory movements cause great movement of the liver, the patient needs to be able to hold his/ her breath when told to. For some patients, this may be very difficult.

Liver biopsy

Percutaneous image-guided biopsy of focal liver lesions is a well-established method for cytological or histological classification [85-92]. In some part of the literature, core biopsy is preferred over fine needle aspiration (FNA) due to the need for a definite histological classification as reported by Stattaus et al. [87].

The complication rate with US-guided percutaneous liver biopsy is low, with an overall complication rate of 0.2%-0.3%. In comparison the complication rate of CT-guided liver biopsy is reported 0.4% in a study by Thanos et al. [93]. Haemorrhage is the most common complication [76,91,94,95]. The complication rate decreases with image guidance [88] and increases in patients with malignancy and chronic active hepatitis [94]. In the initial phase of the study, we considered performing fusion-guided biopsy of liver lesions only visible on CT or MRI. However, we found that the movements of the liver (parallel and rotational shifts) decreased the accuracy of the co-registration, and hereby we risked false negative conclusions. The median size of the lesions in the patient study was 15 mm, thus making even small parallel shifts crucial for a correct diagnosis.

Off-line fusion for planning of radiation therapy

2D and 3D anal endosonography are considered accurate and safe methods for evaluating the anorectum [23-25,27-30,96,97].

Results from image fusion involving TRUS and CT or MRI were promising for planning interstitial brachytherapy for prostate cancer, because TRUS visualizes the prostate gland well but MRI is better for delineating focal lesions and the brachytherapy needles [16-20]. These results have been confirmed by other groups [1,52]

In our department all patients with suspected anal cancer are scanned with 3D endosonography, a method, which had been evaluated by other members of our research group. Due to this and the promising results from image fusion for brachytherapy guidance we were interested in studying image fusion for the radiation therapy treatment of anal cancer. We initially intended to import all 3D-anal endosonography examinations in the dose-planning program in order to direct the radiation therapy more precisely towards the tumour tissue. However, according to the guidelines from the department of radiation oncology and to studies from other groups, the original tumour volume had to be

irradiated without regard to the effect of the external radiation therapy when planning interstitial brachytherapy [97]. In many cases most of the original tumour volume had been eliminated due to the external beam radiation. We could not import the primary staging endosonogram as the perspex rod and the needles were not present at that time, and we needed them for the co-registration procedure and the dose planning. Therefore it was not possible to apply the method in the clinical setting. We did however show that it was possible to perform off-line image-fusion between a non-DICOM standard 3D endosonography examination and CT and PET. Furthermore, it was possible to make an easy-to-use software application in lack of commercial alternatives. Because PET/CT replaced 3D endosonography in the planning of external radiation therapy the method was never tested in larger patient studies.

The approach towards interstitial brachytherapy varies worldwide. In the United States it is rarely used, due to the invasiveness of the treatment so only external beam radiation is used [30]. In Europe interstitial brachytherapy is more widely used but the advantages seem to be limited due to its invasiveness and logistics [97,98]. Further studies are needed to describe if intensity-modulated radiation therapy will be the method of choice in the future [98,99].

Time spent on real-time image fusion

We found that the method was more time consuming than an ordinary US, due to the set-up with the magnetic positioning system, the reading of the previously recorded CT or MRI and the co-registration procedure. In our first phantom study (study I), we measured the time spent per co-registration procedure. This decreased as the examiner became increasingly familiar with the co-registration method. It increased again when the procedure changed from points to planes, thereby becoming new to the examiner. This was apparent even though our data did not support a characteristic learning curve for the two observers. In this first phantom study, the co-registration procedure, without connection of the hardware and reading of the CD, lasted between 1.5 minutes and 4 minutes on average. However, this was in an ideal setting with several easily identifiable points and planes and without any patient motion. These results are in accordance with other groups': Crocetti et al. reported that they spent 3-5 minutes on the set-up and the co-registration procedure [60]. Krucker et al. spent 5.25 minutes in total on set-up and co-registration [2].

In our second phantom study (study II), the complete co-registration took about 10 minutes. In this phantom, the co-registration was made from 4 visible spheres and 4 copper threads placed in each corner of the phantom box. This procedure was slightly more difficult than in the first study as the copper threads were only 1.5 mm in diameter, and it was difficult to obtain corresponding points in the spheres. However, there were still no respiratory movements.

In our patient study (study III), we did not measure the time spent on the co-registration procedure but generally it was more time consuming than in the phantoms. For the initial plane co-registration, we used the upper mesenteric artery, the division of the aortic artery or the umbilicus, and the overview in these regions varied a lot between the patients. Furthermore, the finding of common points in the liver afterwards also took some time trying to compensate for parallel and rotational shifts. Nevertheless, it was our impression that the time-spent decreased along the experiment. The time spent on the co-registration procedure has not been reported from any of the liver studies in patients.

For the off-line fusion between US and PET/CT the conversion of the 3D anal endosonogram block to separate image files took approximately 10 minutes and the alignment of the images took approximately 5 minutes.

Undoubtedly, the time spent on the co-registration will decrease as familiarity with the method increases and it will probably still be less time consuming than CT- or MRI-guided biopsies [84].

We have not been able to find any studies reporting the mean time spent on a CEUS of the liver and we did not register the time spent on fusion-guidance in the patients. However, the co-registration was not as readily done in patients as in the phantoms, and it did require some extra time. This extra time spent has to be held against the extra cost for a new CT/ MRI or PET/CT including the extra radiation exposure and the waiting time for the patient. Two recent multi centre studies from France and Germany have shown a lower cost for CEUS compared with CT or MRI [100,101]. In the French study 1034 liver lesions were examined with CEUS and related to a gold standard being contrast-enhanced CT or MRI or biopsy in the cases where it was obtained. Only the cost for the contrast agent was considered in the economical evaluation and not the extra time needed for additional examinations.

Relation between CEUS and image fusion involving US

According to European Guidelines for CEUS, CEUS is the method of choice in liver imaging when there is incidental findings on routine US, lesions or suspected lesions in a patient with a known history of malignancy, patients with inconclusive MRI/CT results or cytology/histology results [13]. In order to study the potential benefits from image-fusion involving real-time US we decided to apply fusion-guidance before adding CEUS in our study. In doing so we discovered that fusion-guidance aided us in focusing CEUS especially in the patients with suspected metastases from neuroendocrine tumours.

No other studies have compared the application of fusion-guidance and CEUS, but the two methods will probably complement each other in the future.

Reproducibility

None of the studies describing image fusion involving real-time US for liver application has measured the reproducibility of the method. However, the user dependency of US is frequently referred [101].

We considered the reproducibility of the method in all our studies. In our first study (study I) two different observers did the co-registrations; one had prior knowledge to the system the other had not. We compared their accuracies by analysis of variance and they did not differ significantly. In our second study (study II) three observers with the same experience level took all biopsies and their rate of success did not differ significantly. From these results we conclude that the method was reproducible in a phantom. Furthermore the measured accuracies and the time spent on the co-registrations were in accordance with results from other groups. We have not used Kappa statistics, as the data we compared were not categorical and data were not readily transformed into categorical data [102].

In our patient study (study III), two experienced physicians did all examinations together in order to improve the examinations regarding time-spent and accuracy of the co-registration. We did

not compare different observers in this study as it would have required a much larger number of patients and because in some occasions quite some time passed between we used the system. If the two observers should each have performed the examinations independently, a much longer time would have been required for each examination and the co-registrations would probably not have been as good. Of course when relying on anatomical landmarks the method depends on the user's ability to locate exactly the same point in two data sets from different imaging modalities, making the method user-dependent.

In the study on off-line image fusion for 3D anal endosonography (study IV), we did not consider reproducibility, as we never reached the clinical testing. However, the software was very user friendly, thus the reproducibility would depend only on the user's ability to find one corresponding point in the different data sets apart from the perspex rod.

Strengths and limitations

The studies included in this PhD-thesis each have their strengths and limitations.

In the first study (study I) we had a high number of co-registrations in a phantom optimal for both point- and plane co-registration. We optimized the setup to avoid interference on the magnetic positioning system and systematic errors. Further, the purpose of this study was focused on the co-registration procedure. We tried to consider reproducibility and learning curves by having two different observers perform the co-registrations. The limitations of this study were that it only described accuracies in a phantom, which was made for this study on co-registration, as it contained several well-defined points and planes.

In the second study (study II) we also had a high number of biopsies made by three different observers in order to increase the statistical significance and compare the rate of success between the observers. In this study we did not focus on the co-registration procedure except that we made sure the co-registration was accurate before beginning the biopsy procedure. We tested two different systems, which did not perform significantly different. The limitations were that it was a phantom study and that we only performed biopsy of structures lying in a maximal depth of 10 cm. This distance would presumably be longer in patients.

In the third study (study III) we decided to use the method only in selected patients, where the lesion was considered difficult to visualize judging from the previously recorded CT or MRI. We made follow-up on all patients in order to obtain the "true diagnosis". The limitation of this study was the lack of accuracy measurement, which was due to difficulties in deciding which point and in which plane it should be measured. Furthermore the co-registration could be accurate in one of the co-registration points but not for the lesion. Including more patients and comparing different observers could also have improved this study, but we chose to focus on lesions that could be difficult to visualize judging from the CT or MRI. Testing the use of external markers would also have been relevant, but would be difficult to do in our hospital setting, as we did not know which patients have lesions that were difficult to delineate by US and required biopsy. It would also be necessary with immediate interpretation of the CT images and immediate US in order not to move the external markers.

In the fourth study (study IV) the main limitation is naturally the lack of clinical testing - we only report one case.

Perspectives

When we planned the studies described in this thesis, two commercial US systems with incorporated software for fusion imaging were available from Esaote and Hitachi. Now it is also incorporated in the latest system from GE, and in the future more vendors will probably incorporate such software in their systems.

We found the method useful for liver lesions but it will probably also be of use for areas with poor US overview, i.e. abscesses containing air.

In the future, hopefully triple modality fusion between PET/CT and US will be possible, as some lesions are still only visible with the application of PET. Due to limited data capacity a PET/CT fusion is only possible to see in its entire length on a workstation in connection with the scanner. The PET or CT examination can currently only be stored separately in DICOM on a CD. It is not possible to use the PET part separately due to its lack of anatomical landmarks for the co-registration with US. If it was possible to get an entire PET/CT dataset in the standardized DICOM format, it could be loaded into the US system and be used as guidance. The advantages of a successful triple modality co-registration between PET/CT and US could be the detection and biopsy of tumours at an earlier stage and thereby the possibility of earlier treatment of several cancer types. In regions where several closely related lymph nodes are enlarged but only some are PET-positive the method will be useful for biopsy guidance of the suspect lymph node. Also in tumours with necrotic areas, where PET will mark the vital tumour tissue, a representative biopsy containing vital tumour will be available using the method.

Fusion of real-time US images with previously recorded US images is possible using the prototype system described in this thesis. Unfortunately the testing of it was beyond the scope of this thesis. However, fusion of previously recorded US image with real-time US images could be useful in the monitoring of treatment in arthritis, in vascular diseases and in lymphomas. It could also be useful in the follow-up of paediatric cancers and cancers in young patients, because US causes no ionizing, thus having an advantage over CT.

Further studies describing standardized methods for co-registering the images in different regions are needed in order to optimize the co-registration procedure and to gain knowledge on which structures can be used in different regions.

CONCLUSION

We have successfully tested a method for image fusion between real-time US and CT or MRI in phantoms and patients where liver lesions were suspected. From our phantom studies we concluded that the method was accurate, with accuracies comparable to those obtained from PET/CT, considering the co-registration of the images. The method was also accurate for obtaining biopsy of lesions that were only visible on CT or MRI in a phantom. We successfully continued our studies in patients, where we were able to delineate an increasing number of lesions compared with conventional B-mode US and we were able to focus our CEUS by means of the method.

In our opinion, the method is a promising new tool for US-guided intervention, which will probably gain widespread use in the future.

REFERENCES

1 Kaplan ID, Meskell P, Oldenburg NE, Saltzman B, Kearney GP, Holupka EJ. Real-time computed tomography dosimetry during ultrasound-guided brachytherapy for prostate cancer. Brachytherapy 2006;5(3):147-51.

2 Krucker J, Xu S, Glossop N, Viswanathan A, Borgert J, Schulz H, et al. Electromagnetic tracking for thermal ablation and biopsy guidance: clinical evaluation of spatial accuracy. J Vasc Interv Radiol 2007;18(9):1141-50.

3 Lindseth F, Ommedal S, Bang J, Unsgård G, Hernes TAN. Image fusion of ultrasound and MRI as an aid for assessing anatomical shifts and improving overview and interpretation in ultrasound guided neurosurgery. International Congress Series 2001;1230:254-60.

4 Maintz JB, Viergever MA. A survey of medical image registration. Med Image Anal 1998;2(1):1-36.

5 Ewertsen C, Grossjohann HS, Nielsen MB. Image fusion involving ultrasound. Ultraschall Med 2006;27(2):128-9.

6 Ewertsen C, Nielsen KR, Henriksen BM, Torp-Pedersen S, Nielsen MB. [Image fusion with ultrasound]. Ugeskr Laeger 2009;171(13):1069.

7 Diagnostic Ultrasound. 2nd ed. New York: Informa Healthcare; 2008.

8 Basics of Clinical Ultrasound. 1 ed. Hvidovre: 2005.

9 Basic and new Aspects of Gastrointestinal Ultrasonography. Singapore: World Scientific Publishing Co; 2005.

10 Blomley M, Claudon M, Cosgrove D. WFUMB Safety Symposium on Ultrasound Contrast Agents: clinical applications and safety concerns. Ultrasound Med Biol 2007;33(2):180-6.

11 Cosgrove D. Ultrasound contrast agents: an overview. Eur J Radiol 2006;60(3):324-30.

12 Solbiati L, Martegani A, Leen E, Correas JM, Burns PN, Becker D. Contrast-Enhanced Ultrasound of Liver Diseases. Milano: Springer-Verlag; 2003.

13 Claudon M, Cosgrove D, Albrecht T, Bolondi L, Bosio M, Calliada F, et al. Guidelines and good clinical practice recommendations for contrast enhanced ultrasound (CEUS) - update 2008. Ultraschall Med 2008;29(1):28-44.

14 Lencioni R. Impact of European Federation of Societies for Ultrasound in Medicine and Biology (EFSUMB) guidelines on the use of contrast agents in liver ultrasound. Eur Radiol 2006;16(7):1610-3.

15 Strobel D, Seitz K, Blank W, Schuler A, Dietrich C, von HA, et al. Contrast-enhanced ultrasound for the characterization of focal liver lesions--diagnostic accuracy in clinical practice (DEGUM multicenter trial). Ultraschall Med 2008;29(5):499-505.

16 Fuller DB, Jin H, Koziol JA, Feng AC. CT-ultrasound fusion prostate brachytherapy: a dynamic dosimetry feedback and improvement method. A report of 54 consecutive cases. Brachytherapy 2005;4(3):207-16.

17 Holupka EJ, Kaplan ID, Burdette EC, Svensson GK. Ultrasound image fusion for external beam radiotherapy for prostate cancer. Int J Radiat Oncol Biol Phys 1996;35(5):975-84.

18 Reynier C, Troccaz J, Fourneret P, Dusserre A, Gay-Jeune C, Descotes JL, et al. MRI/TRUS data fusion for prostate brachytherapy. Preliminary results. Med Phys 2004;31(6):1568-75.

19 Steggerda M, Schneider C, van HM, Zijp L, Moonen L, van der PH. The applicability of simultaneous TRUS-CT imaging for the evaluation of prostate seed implants. Med Phys 2005;32(7):2262-70.

20 Kaplan I, Oldenburg NE, Meskell P, Blake M, Church P, Holupka EJ. Real time MRI-ultrasound image guided stereotactic prostate biopsy. Magn Reson Imaging 2002;20(3):295-9.

21 Wild JJ, Reid JM. Diagnostic use of ultrasound. Br J Phys Med 1956;19(11):248-57.

22 Dragsted J, Gammelgaard J. Endoluminal ultrasonic scanning in the evaluation of rectal cancer: a preliminary report of 13 cases. Gastrointest Radiol 1983;8(4):367-9.

23 Nielsen MB, Qvitzau S, Pedersen JF, Christiansen J. Endosonography for preoperative staging of rectal tumours. Acta Radiol 1996;37(5):799-803.

24 Nielsen MB. Endosonography of the anal sphincter muscles in healthy volunteers and in patients with defecation disorders. Acta Radiol Suppl 1998;416:1-21.

25 Engin G. Endosonographic imaging of anorectal diseases. J Ultrasound Med 2006;25(1):57-73.

26 Felt-Bersma RJ. Endoanal ultrasound in benign anorectal disorders: clinical relevance and possibilities. Expert Rev Gastroenterol Hepatol 2008;2(4):587-606.

27 Saranovic D, Barisic G, Krivokapic Z, Masulovic D, Djuric-Stefanovic A. Endoanal ultrasound evaluation of anorectal diseases and disorders: technique, indications, results and limitations. Eur J Radiol 2007;61(3):480-9.

28 Christensen AF, Nyhuus B, Nielsen MB. Interobserver and intraobserver variation of two-dimensional and three-dimensional anal endosonography in the evaluation of recurrent anal cancer. Dis Colon Rectum 2009;52(3):484-8.

29 Christensen AF, Nielsen BM, Engelholm SA. Three-dimensional endoluminal ultrasound-guided interstitial brachytherapy in patients with anal cancer. Acta Radiol 2008;49(2):132-7.

30 Engstrom PF. NCCN practice guidelines in oncology v.1.2009 Anal Carcinoma. 2009.

31 Roed H, Engelholm SA, Svendsen LB, Rosendal F, Olsen KJ. Pulsed dose rate (PDR) brachytherapy of anal carcinoma. Radiother Oncol 1996;41(2):131-4.

32 Porter BC, Rubens DJ, Strang JG, Smith J, Totterman S, Parker KJ. Three-dimensional registration and fusion of ultrasound and MRI using major vessels as fiducial markers. IEEE Trans Med Imaging 2001;20(4):354-9.

33 Penney GP, Blackall JM, Hamady MS, Sabharwal T, Adam A, Hawkes DJ. Registration of freehand 3D ultrasound and magnetic resonance liver images. Med Image Anal 2004;8(1):81-91.

34 Cothren RM, Shekhar R, Tuzcu EM, Nissen SE, Cornhill JF, Vince DG. Three-dimensional reconstruction of the coronary artery wall by image fusion of intravascular ultrasound and bi-plane angiography. Int J Card Imaging 2000;16(2):69-85.

35 Slager CJ, Wentzel JJ, Schuurbiers JC, Oomen JA, Kloet J, Krams R, et al. True 3-dimensional reconstruction of coronary arteries in patients by fusion of angiography and IVUS (ANGUS) and its quantitative validation. Circulation 2000;102(5):511-6.

36 Wahle A, Prause GP, von BC, Erbel R, Sonka M. Fusion of angiography and intravascular ultrasound in vivo: establishing the absolute 3-D frame orientation. IEEE Trans Biomed Eng 1999;46(10):1176-80.

37 Wahle A, Prause PM, DeJong SC, Sonka M. Geometrically correct 3-D reconstruction of intravascular ultrasound images by fusion with biplane angiography--methods and validation. IEEE Trans Med Imaging 1999;18(8):686-99.

38 Wahle A, Olszewski ME, Sonka M. Interactive virtual endoscopy in coronary arteries based on multimodality fusion. IEEE Trans Med Imaging 2004;23(11):1391-403.

39 Wahle A, Lopez JJ, Olszewski ME, Vigmostad SC, Chandran KB, Rossen JD, et al. Plaque development, vessel curvature, and wall shear stress in coronary arteries assessed by X-ray angiography and intravascular ultrasound. Med Image Anal 2006;10(4):615-31.

40 Slomka PJ, Mandel J, Downey D, Fenster A. Evaluation of voxel-based registration of 3-D power Doppler ultrasound and 3-D magnetic resonance angiographic images of carotid arteries. Ultrasound Med Biol 2001;27(7):945-55.

41 Molloy JA, Oldham SA. Benchmarking a novel ultrasound-CT fusion system for respiratory motion management in radiotherapy: assessment of spatio-temporal characteristics and comparison to 4DCT. Med Phys 2008;35(1):291-300.

42 Schlaier JR, Warnat J, Dorenbeck U, Proescholdt M, Schebesch KM, Brawanski A. Image fusion of MR images and real-time ultrasonography: evaluation of fusion accuracy combining two commercial instruments, a neuronavigation system and a ultrasound system. Acta Neurochir (Wien) 2004;146(3):271-6.

43 Tirakotai W, Miller D, Heinze S, Benes L, Bertalanffy H, Sure U. A novel platform for image-guided ultrasound. Neurosurgery 2006;58(4):710-8.

44 Lindner D, Trantakis C, Renner C, Arnold S, Schmitgen A, Schneider J, et al. Application of intraoperative 3D ultrasound during navigated tumor resection. Minim Invasive Neurosurg 2006;49(4):197-202.

45 Miller D, Heinze S, Tirakotai W, Bozinov O, Surucu O, Benes L, et al. Is the image guidance of ultrasonography beneficial for neurosurgical routine? Surg Neurol 2007;67(6):579-87.

46 Wein W, Roper B, Navab N. Automatic registration and fusion of ultrasound with CT for radiotherapy. Med Image Comput Comput Assist Interv Int Conf Med Image Comput Comput Assist Interv 2005;8(Pt 2):303-11.

47 Ewertsen C, Ellegaard K, Boesen M, Torp-Pedersen S, Bachmann NM. Comparison of two co-registration methods for real-time ultrasonography fused with MRI: a phantom study. Ultraschall Med 2010;31(3):296-301.

48 Ewertsen C, Grossjohann HS, Nielsen KR, Torp-Pedersen S, Nielsen MB. Biopsy guided by real-time sonography fused with MRI: a phantom study. AJR Am J Roentgenol 2008;190(6):1671-4.

49 O'Neill BD, Salerno G, Thomas K, Tait DM, Brown G. MR vs CT imaging: low rectal cancer tumour delineation for three-dimensional conformal radiotherapy. Br J Radiol 2009;82(978):509-13.

50 Sun MR, Smith MP, Kane RA. Current techniques in imaging of fistula in ano: three-dimensional endoanal ultrasound and magnetic resonance imaging. Semin Ultrasound CT MR 2008;29(6):454-71.

51 Wein W, Brunke S, Khamene A, Callstrom MR, Navab N. Automatic CT-ultrasound registration for diagnostic imaging and image-guided intervention. Med Image Anal 2008;12(5):577-85.

52 Xu S, Kruecker J, Guion P, Glossop N, Neeman Z, Choyke P, et al. Closed-loop control in fused MR-TRUS image-guided prostate biopsy. Med Ima-

ge Comput Comput Assist Interv Int Conf Med Image Comput Comput Assist Interv 2007;10(Pt 1):128-35.
53 Forster GJ, Laumann C, Nickel O, Kann P, Rieker O, Bartenstein P. SPET/CT image co-registration in the abdomen with a simple and cost-effective tool. Eur J Nucl Med Mol Imaging 2003;30(1):32-9.
54 Pichler BJ, Wehrl HF, Kolb A, Judenhofer MS. Positron emission tomography/magnetic resonance imaging: the next generation of multimodality imaging? Semin Nucl Med 2008;38(3):199-208.
55 Schlemmer HP, Pichler BJ, Schmand M, Burbar Z, Michel C, Ladebeck R, et al. Simultaneous MR/PET imaging of the human brain: feasibility study. Radiology 2008;248(3):1028-35.
56 Wehrl HF, Judenhofer MS, Wiehr S, Pichler BJ. Pre-clinical PET/MR: technological advances and new perspectives in biomedical research. Eur J Nucl Med Mol Imaging 2009;36 Suppl 1:S56-S68.
57 Lavely WC, Scarfone C, Cevikalp H, Li R, Byrne DW, Cmelak AJ, et al. Phantom validation of coregistration of PET and CT for image-guided radiotherapy. Med Phys 2004;31(5):1083-92.
58 Beyer T, Townsend DW, Brun T, Kinahan PE, Charron M, Roddy R, et al. A combined PET/CT scanner for clinical oncology. J Nucl Med 2000;41(8):1369-79.
59 Goerres GW, Kamel E, Heidelberg TN, Schwitter MR, Burger C, von Schulthess GK. PET-CT image co-registration in the thorax: influence of respiration. Eur J Nucl Med Mol Imaging 2002;29(3):351-60.
60 Crocetti L, Lencioni R, Debeni S, See TC, Pina CD, Bartolozzi C. Targeting liver lesions for radiofrequency ablation: an experimental feasibility study using a CT-US fusion imaging system. Invest Radiol 2008;43(1):33-9.
61 Hirooka M, Iuchi H, Kumagi T, Shigematsu S, Hiraoka A, Uehara T, et al. Virtual sonographic radiofrequency ablation of hepatocellular carcinoma visualized on CT but not on conventional sonography. AJR Am J Roentgenol 2006;186(5 Suppl):S255-S260.
62 Minami Y, Kudo M, Chung H, Inoue T, Takahashi S, Hatanaka K, et al. Percutaneous radiofrequency ablation of sonographically unidentifiable liver tumors. Feasibility and usefulness of a novel guiding technique with an integrated system of computed tomography and sonographic images. Oncology 2007;72 Suppl 1:111-6.
63 Minami Y, Chung H, Kudo M, Kitai S, Takahashi S, Inoue T, et al. Radiofrequency ablation of hepatocellular carcinoma: value of virtual CT sonography with magnetic navigation. AJR Am J Roentgenol 2008;190(6):W335-W341.
64 Wein W, Khamene A, Clevert DA, Kutter O, Navab N. Simulation and fully automatic multimodal registration of medical ultrasound. Med Image Comput Comput Assist Interv Int Conf Med Image Comput Comput Assist Interv 2007;10(Pt 1):136-43.
65 Wendler T, Feuerstein M, Traub J, Lasser T, Vogel J, Daghighian F, et al. Real-time fusion of ultrasound and gamma probe for navigated localization of liver metastases. Med Image Comput Comput Assist Interv Int Conf Med Image Comput Comput Assist Interv 2007;10(Pt 2):252-60.
66 Gupta S, Madoff DC. Image-guided percutaneous needle biopsy in cancer diagnosis and staging. Tech Vasc Interv Radiol 2007;10(2):88-101.
67 Rasmussen SN, Holm HH, Kristensen JK, Barlebo H. Ultrasonically-guided liver biopsy. Br Med J 1972;2(5812):500-2.
68 Kristensen JK, Holm HH, Rasmussen SN, Barlebo H. Ultrasonically guided percutaneous puncture of renal masses. Scand J Urol Nephrol 1972;6:Suppl-56.
69 Pedersen JF, Hancke S, Kristensen JK. Renal carbuncle: antibiotic therapy governed by ultrasonically guided aspiration. J Urol 1973;109(5):777-8.
70 Pedersen JF. Percutaneous nephrostomy guided by ultrasound. J Urol 1974;112(2):157-9.
71 Gammelgaard J, Jensen F. Ultrasonically guided celiac axis block in intractable pain. Int.Congress Series, Excerpta Medica 1981; 547: 106.
72 Karstrup S, Nolsoe C, Brabrand K, Nielsen KR. Ultrasonically guided percutaneous drainage of breast abscesses. Acta Radiol 1990;31(2):157-9.
73 Nielsen MB, Pedersen JF, Hald J, Christiansen J. Recurrent extraluminal rectal carcinoma: transrectal biopsy under sonographic guidance. AJR Am J Roentgenol 1992;158(5):1025-7.
74 Nielsen MB, Torp-Pedersen S. Sonographically guided transrectal or transvaginal one-step catheter placement in deep pelvic and perirectal abscesses. AJR Am J Roentgenol 2004;183(4):1035-6.
75 Jørgensen J. Ultralyddiagnostik i Danmark - en historisk oversigt. Bibliotek for Læger; 2003.
76 Buscarini E. Review of interventional ultrasound in the abdomen: safety first. Ultraschall Med. 2004; 24: 11-15.
77 Howard MH, Nelson RC, Paulson EK, Kliewer MA, Sheafor DH. An electronic device for needle placement during sonographically guided percutaneous intervention. Radiology 2001;218(3):905-11.
78 Schweiger GD, Brown BP, Pelsang RE, Dhadha RS, Barloon TJ, Wang G. CT fluoroscopy: technique and utility in guiding biopsies of transiently enhancing hepatic masses. Abdom Imaging 2000;25(1):81-5.
79 Liermann D, Kickuth R. CT fluoroscopy-guided abdominal interventions. Abdom Imaging 2003;28(1):129-34.
80 Das CJ, Goenka AH, Srivastava DN. MR-guided abdominal biopsy using a 1.5-Tesla closed system: a feasibility study. Abdom Imaging 2009.
81 Stattaus J, Maderwald S, Baba HA, Gerken G, Barkhausen J, Forsting M, et al. MR-guided liver biopsy within a short, wide-bore 1.5 Tesla MR system. Eur Radiol 2008;18(12):2865-73.
82 Kariniemi J, Blanco SR, Ojala R, Tervonen O. MRI-guided abdominal biopsy in a 0.23-T open-configuration MRI system. Eur Radiol 2005;15(6):1256-62.
83 Lu DS, Lee H, Farahani K, Sinha S, Lufkin R. Biopsy of hepatic dome lesions: semi-real-time coronal MR guidance technique. AJR Am J Roentgenol 1997;168(3):737-9.
84 Kliewer MA, Sheafor DH, Paulson EK, Helsper RS, Hertzberg BS, Nelson RC. Percutaneous liver biopsy: a cost-benefit analysis comparing sonographic and CT guidance. AJR Am J Roentgenol 1999;173(5):1199-202.
85 Chojniak R, Isberner RK, Viana LM, Yu LS, Aita AA, Soares FA. Computed tomography guided needle biopsy: experience from 1,300 procedures. Sao Paulo Med J 2006;124(1):10-4.
86 Sheafor DH, Paulson EK, Simmons CM, DeLong DM, Nelson RC. Abdominal percutaneous interventional procedures: comparison of CT and US guidance. Radiology 1998;207(3):705-10.
87 Stattaus J, Kuehl H, Ladd S, Schroeder T, Antoch G, Baba HA, et al. CT-guided biopsy of small liver lesions: visibility, artifacts, and corresponding diagnostic accuracy. Cardiovasc Intervent Radiol 2007;30(5):928-35.
88 Winter TC, Lee FT, Jr., Hinshaw JL. Ultrasound-guided biopsies in the abdomen and pelvis. Ultrasound Q 2008;24(1):45-68.
89 Yu SC, Liew CT, Lau WY, Leung TW, Metreweli C. US-guided percutaneous biopsy of small (< or = 1-cm) hepatic lesions. Radiology 2001;218(1):195-9.
90 Welch TJ, Sheedy PF, Johnson CD, Johnson CM, Stephens DH. CT-guided biopsy: prospective analysis of 1,000 procedures. Radiology 1989;171(2):493-6.
91 Garcia-Tsao G, Boyer JL. Outpatient liver biopsy: how safe is it? Ann Intern Med 1993;118(2):150-3.
92 Buscarini L, Fornari F, Bolondi L, Colombo P, Livraghi T, Magnolfi F, et al. Ultrasound-guided fine-needle biopsy of focal liver lesions: techniques, diagnostic accuracy and complications. A retrospective study on 2091 biopsies. J Hepatol 1990;11(3):344-8.
93 Thanos L, Zormpala A, Papaioannou G, Malagari K, Brountzos E, Kelekis D. Safety and efficacy of percutaneous CT-guided liver biopsy using an 18-gauge automated needle. Eur J Intern Med 2005;16(8):571-4.
94 Piccinino F, Sagnelli E, Pasquale G, Giusti G. Complications following percutaneous liver biopsy. A multicentre retrospective study on 68,276 biopsies. J Hepatol 1986;2(2):165-73.
95 Van Thiel DH, Gavaler JS, Wright H, Tzakis A. Liver biopsy. Its safety and complications as seen at a liver transplant center. Transplantation 1993;55(5):1087-90.
96 Christensen AF, Nielsen MB, Engelholm SA, Roed H, Svendsen LB, Christensen H. Three-dimensional anal endosonography may improve staging of anal cancer compared with two-dimensional endosonography. Dis Colon Rectum 2004;47(3):341-5.
97 Doniec JM, Schniewind B, Kovacs G, Kahlke V, Loehnert M, Kremer B. Multimodal therapy of anal cancer added by new endosonographic-guided brachytherapy. Surg Endosc 2006;20(4):673-8.
98 Oehler-Janne C, Seifert B, Lutolf UM, Studer G, Glanzmann C, Ciernik IF. Clinical outcome after treatment with a brachytherapy boost versus external beam boost for anal carcinoma. Brachytherapy 2007;6(3):218-26.
99 Milano MT, Jani AB, Farrey KJ, Rash C, Heimann R, Chmura SJ. Intensity-modulated radiation therapy (IMRT) in the treatment of anal cancer: toxicity and clinical outcome. Int J Radiat Oncol Biol Phys 2005;63(2):354-61.
100 Giesel FL, Delorme S, Sibbel R, Kauczor HU, Krix M. [Contrast-enhanced ultrasound for the characterization of incidental liver lesions - an economical evaluation in comparison with multi-phase computed tomography]. Ultraschall Med 2009;30(3):259-68.
101 Tranquart F, Correas JM, Ladam M, V, Manzoni P, Vilgrain V, Aube C, et al. [Real-time contrast-enhanced ultrasound in the evaluation of focal liver lesions: diagnostic efficacy and economical issues from a French multicentric study]. J Radiol 2009;90(1 Pt 2):109-22.
102 Altman DG. Practical statistics for medical research. 1st ed. London: Chapman & Hall; 1999.